Basic Propulsion Characteristics of the Superconducting-Permanent Magnet Hybrid Conveyance System

S. Ohashi & D. Dodo
Department of Electrical Engineering and Computer Sciences, Kansai University, Osaka, Japan

ABSTRACT: We have developed the levitation and guidance system with permanent magnet and high temperature bulk super conductor. Additional magnet is introduced in the carrier to realize the hybrid system. Basic levitation characteristics are measured. Propulsion method for this hybrid levitation system is considered. To have the lager thrust force, we proposed the permanent magnet rail with electromagnets. This propulsion magnetic rail shows better thrust characteristics than previous one.

1 INTRODUCTION

The noise, friction and vibration are caused in conventional wheel support system. Therefore it is very difficult to adapt it to the system operated under the special environment (for example, clean room application) or high speed operation. Realization of contact less support is expected to solve them, and magnetically levitated conveyance system has been developed (Moon 1994) (Cardwell et. al. 1997).

In this system, pining force of high temperature super conductor (HTSC) is used for the levitation and guidance (Ohashi et. al. 1999). This system realizes contact-less levitation without control. To increase levitation force, repulsive force of permanent magnet is introduced. We have developed magnetically levitated system with the permanent magnet rail and the carrier with bulk HTSCs. Additional permanent magnets are introduced under the load stage of the carrier. We have realized stable levitation with various load. In this paper, method of the propulsion for this hybrid conveyance system is considered. In the hybrid conveyance system, we adopted repulsive force by the permanent magnet between rail and the load stage, and levitation and guidance one by pining force of the HTSC in the carrier. We propose the following propulsion method. Electromagnets are installed on the carrier. Repulsive force of the electromagnets changes gradient of the carrier, and angle of electromagnet is changed and their repulsive force is used directly for propulsion. To get more propulsion force, we install electromagnets on a rail instead of the carrier. Interaction between the electromagnet and the permanent magnet of the load stage in the carrier is used for propulsion force. Influence of the propulsion system on the levitation characteristics is shown. Basic propulsion characteristics are discussed.

2 EXPERIMENTAL DEVICE

Figure 1 shows the experimental device(Ohashi et. al. 2001). The carrier consists of the frame and the load stage with permanent magnet. The load stage can move freely for vertical direction. On the frame, the HTSC is installed. Figure 2 shows magnetic rail. The rail on the ground is made of neodymium type permanent magnet and back iron.

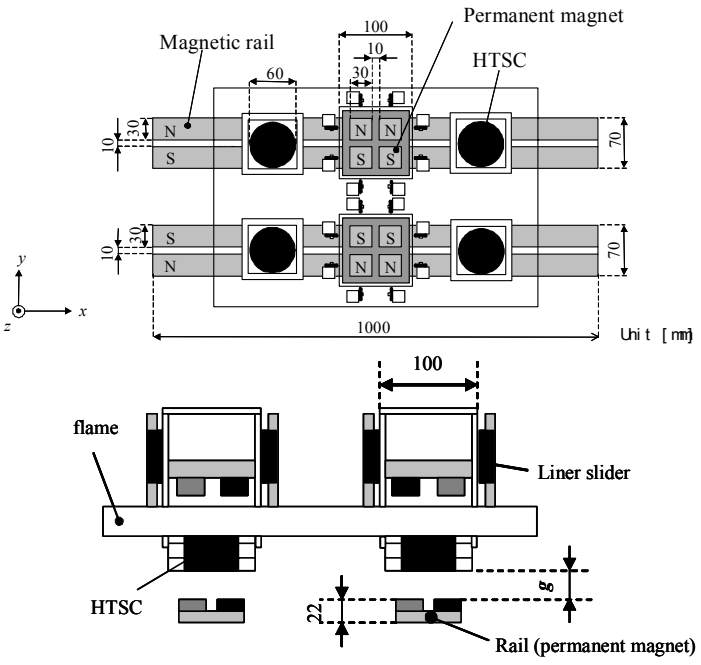

Figure 1: Experimental device.

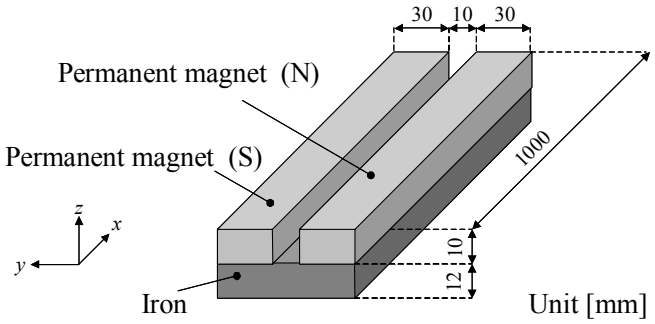

Figure 2: Magnetic rail.

This configuration is decided as follow; when the carrier levitates at air gap = 3 mm, HTSC catches flux from the permanent magnet most effectively. The flux from the permanent magnet rail is pined by the HTSC, and pining force is obtained. As a result, levitation and guidance force of the carrier are given. Pining force is also used to support weight of the frame. Figure 3 shows the load stage in the carrier. The load stage is set on the center of the frame. This is fixed to the frame by liner sliders, and moves only for vertical direction. Repulsive force of the permanent magnet is used to support weight of the load. When the load becomes heavier, vertical position of the load stage goes down to the rail to increase repulsive force. So the carrier can support various weight of load without changing levitation gap of the carrier frame. Table 1 shows specification for permanent magnet. Figure 4 shows the dimension of the HTSC. Table 2 shows specification for the HTSC. Four bulk HTSC are used.

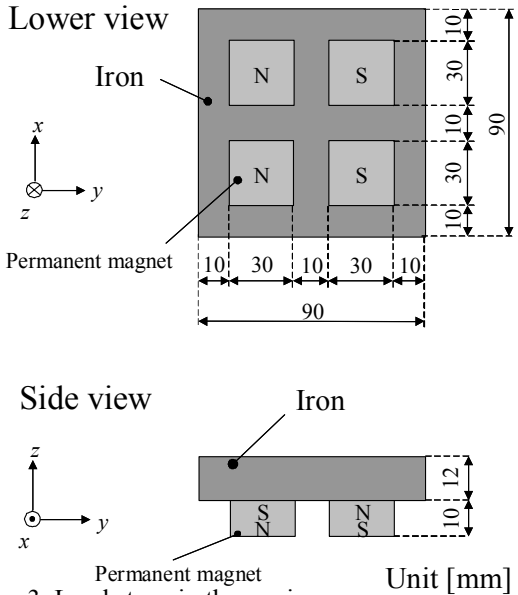

Figure 3. Load stage in the carrier.

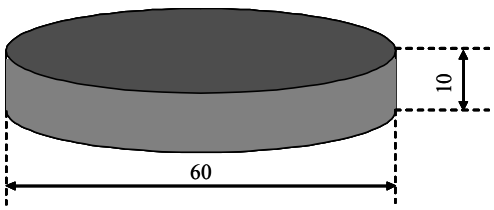

Figure 4: Bulk HTSC.

Table 1: Specifications for permanent magnet.

Dimension	30 mm X 10 mm
Surface flux density	1.34T
Shape	Rectangular solid
Material	Neodymium

Table 2. Specifications for HTSC.

Dimension	φ 60 X10 mm
Critical temperature	91K
Shape	Column
HTSC Type	YBaCuO

The HTSC is indirectly cooled about ten minutes by liquid nitrogen. Then the HTSC is moved to the case which is set on the carrier flame. Then a spacer (made of acrylic board) is put between the HTSC and surface of the rail. The spacer is used to keep levitation gap until flux of the permanent magnet is pined. In this time, the flux from the rail on the ground goes through the HTSC. The case for the HTSC is filled with liquid nitrogen. The HTSC is directly cooled about three minutes by liquid nitrogen, and the flux from the rail on the ground is pined by the HTSC. Figure 5 shows the picture of the experimental device. Two pair of magnetic rail and the carrier with four HTSCs and two load stages is shown. This two pair configuration decrease yaw and roll motion of the carrier.

Next method for the propulsion is considered (Dodo et. al. 2005). When we consider cost for propulsion facility, it is better that the carrier has propulsion function than that the rail on the ground has one. We tried to introduce propulsion function on the carrier. Figure 6 shows method for the propulsion by using repulsive force between permanent magnet on the rail and electromagnets on the carrier (Configuration I). The electromagnets are installed on the rear of the frame. The repulsive force of the electromagnet changes gradient of the frame, and thrust force occurs. Figure 7 shows that by changing the gradient of the electromagnets. In this configuration, gradient of the carrier frame is not directly changed (Configuration II). Same as the method by using repulsive force of the electromagnets, electromagnets are installed on the rear of the frame. Its installation angle is changed to increase repulsive force for the propulsion.

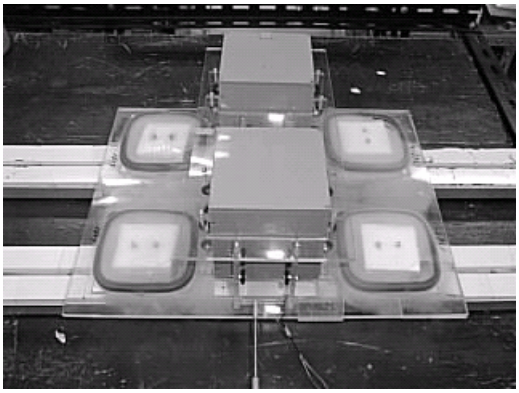

Figure 5: Picture of the experimental device.

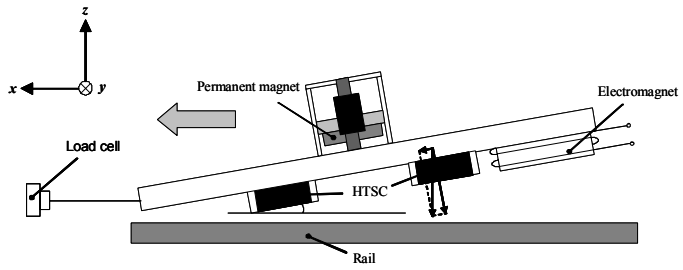

Figure 6: Propulsion method (Configuration I).

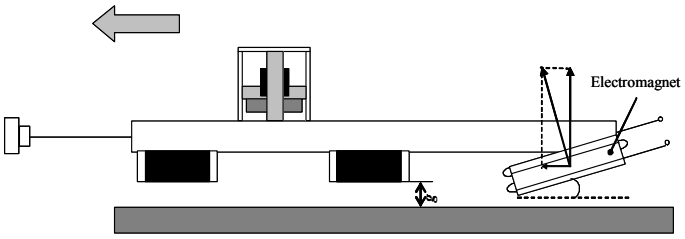

Figure 7: Propulsion method (Configuration II).

3 RESULT

3.1 Initial condition of experiment

Figure 8 shows flux density distribution of the magnetic rail. Center position between north and south pole is defined as $y = 0$. Measurement results from surface 0 to 12 mm for vertical direction are shown. Vertical flux density distribution on y (lateral) axis is measured. The permanent magnet installed under the load stage is same one. Figure 9 shows flux density distribution at the surface of HTSC after field cooling. Result when initial levitation gap (gap when HTSC is field cooled) is shown.

Initial levitation position is considered. The HTSC is cooled with keeping initial levitation gap g_0 by a spacer. Because of the weight of the carrier frame, levitation gap after removing a spacer becomes smaller than g_0. Figure 10 shows relationship between initial gap and initial vertical displacement. Flux pined at HTSC becomes smaller at a larger initial levitation gap. As a result, influence of carrier weight on the vertical displacement becomes large at a larger initial levitation gap.

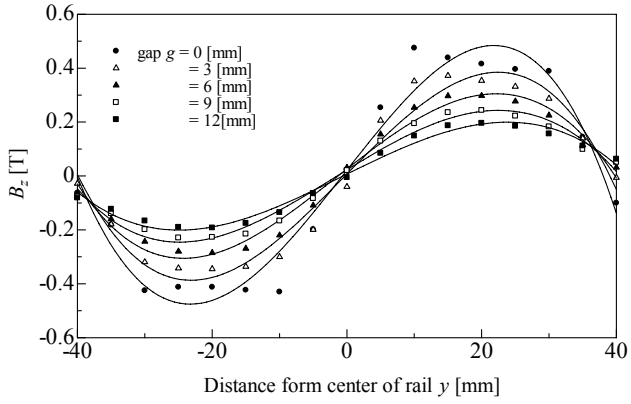

Figure 8: Flux density distribution (permanent magnet).

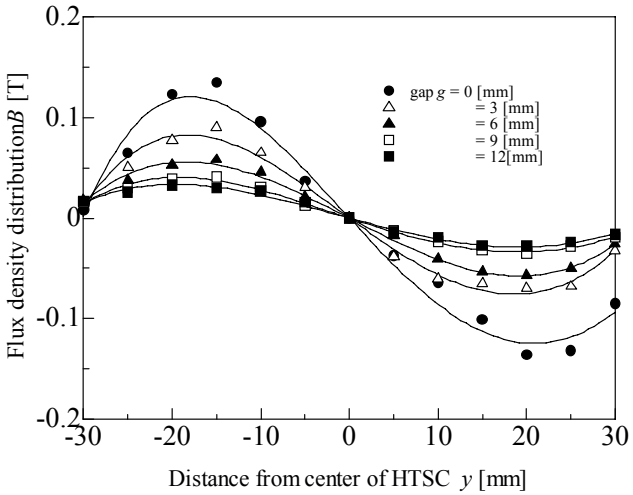

Figure 9: Flux density distribution pined by HTSC.

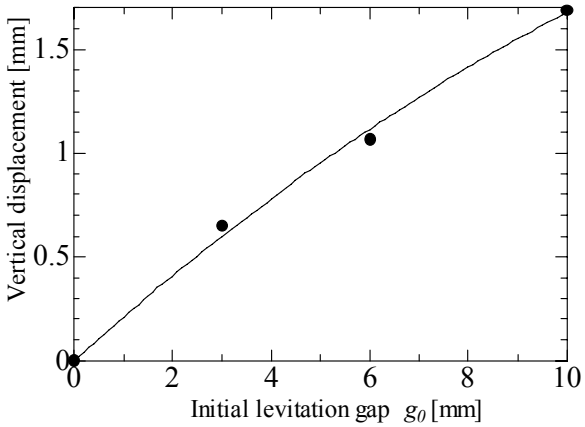

Figure 10: Relationship between initial gap and initial vertical displacement.

3.2 Levitation characteristics

In this system, influence of the load on the carrier frame is almost zero. Vertical displacement of the carrier when step vertical force is added to the load stage is measured. Figure 11 shows influence of weight on the levitation gap of the carrier and the load stage. At $t = 2$ sec, step force $F = 23.5$ N is added to the load stage. Levitation gap of the carrier is 3 mm. As load is supported by the repulsive force between permanent magnet on the rail and under the load stage, there is little influence on the position of the carrier. Because there is some damping factor at a linear slider which fixes the load stage on the carrier frame, oscillation of the stage decreases.

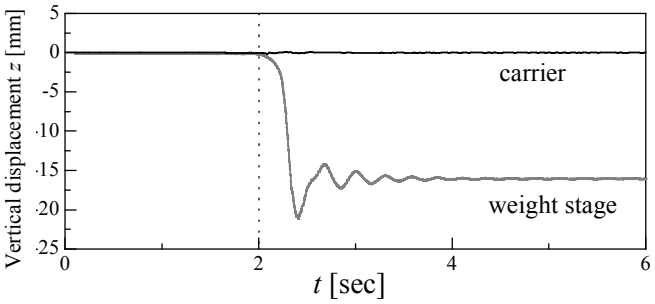

Figure 11: Influence of weight on the levitation gap of the carrier and load stage.

Figure 12 shows load characteristics. Initial levitation gap is 3 mm. Load is added on the load stage, and vertical displacement of the load stage is measured by a laser displacement sensor. Weight of the load stage is 30.6 N. Vertical displacement is measured from this value. Vertical force supporting load weight is generated by repulsive force between permanent magnet. So dw/dz (where w; load weight, z; vertical displacement) becomes small at a larger vertical displacement. In this system, pining force supports unstable lateral force generated by repulsive force. This unstable force becomes larger at a heavier weight, and may cause lateral displacement and rolling motion of the carrier. Because of the mechanical limitation, we can add weight less than 250 N. We confirm stable levitation up to this weight.

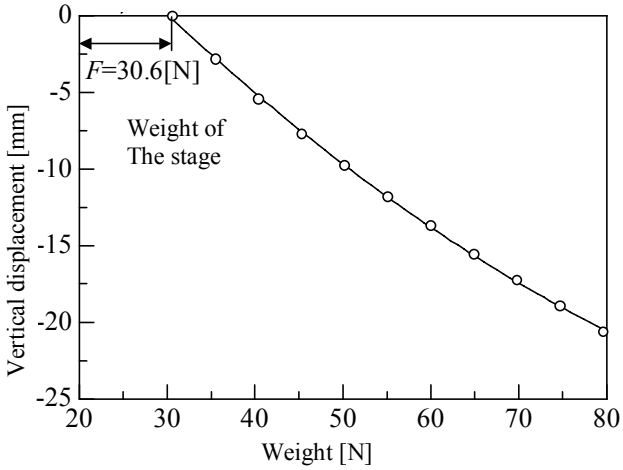

Figure 12: Load characteristics.

3.3 *Influence of the propulsion system*

In Configuration I and II, the carrier is tilted by the electromagnet. The laser sensor is set on rear of the flame, and displacement for the levitating direction is measured. Table 3 shows specifications for electromagnet.

Figure 13 shows dependence of the gap on current of the electromagnet in Configuration I. Result when initial levitation gap is 6, 9 and 12 mm is shown. When levitation gap becomes large, vertical displacement increases. The pining force decreases because of the increment of the gap. In Configuration I, displacement for the levitating direction increases when gap is large, and propulsion force also increases. Simultaneously, instability to the guidance direction increases. The repulsive force decrease because the distance between the electromagnet and the rail on the ground increases when gap is large. Figure 14 shows dependence of the gap on current of the electromagnet in Configuration II. Same characteristics as Figure 13 are observed. Compared with Figure 13, the displacement of the levitating direction is smaller. So, Configuration II has more stability for the guidance direction than Configuration I.

Table 3: Specifications for electromagnet (on the carrier).

Dimension	30 X150 mm
Turn	30
Core	Air core
Diameter	0.8 mm

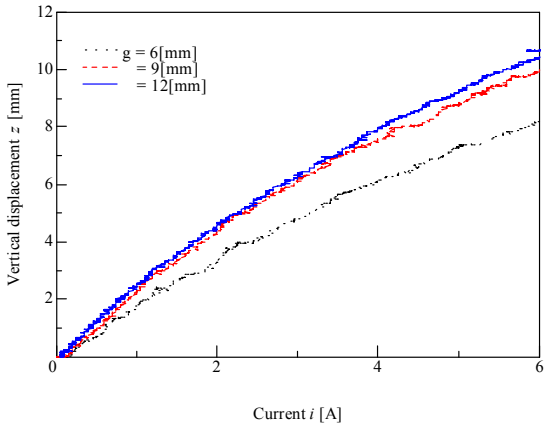

Figure 13: Dependence of the gap on current of the electromagnet in Configuration I.

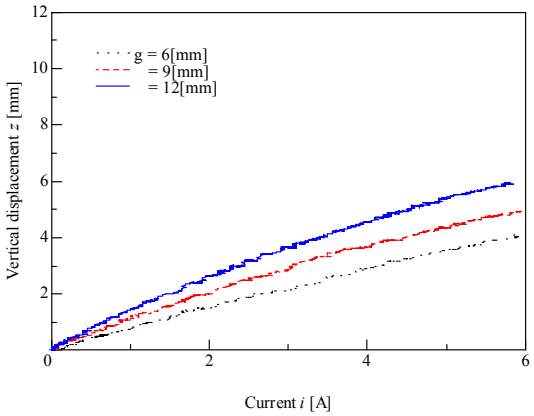

Figure 14: Dependence of the gap on current of the electromagnet in Configuration II.

In both propulsion methods, the carrier inclines its frame. This has influence on pining force of the HTSC. To examine the influence on vertical displacement, the laser sensor is set on center of the flame, and we measure displacement of the levitating direction when the electromagnet turns off after turning on. Figure 15 shows vertical displacement in

Configuration I. The displacement when turning on the electromagnet at t = 1 sec is only 0.5 mm. In addition, there is a little difference from the initial position. From the result, there is a little influence on pining force of the HTSC. Same measurement results are given in Configuration II.

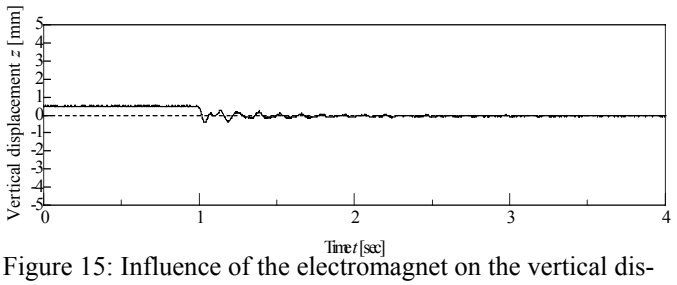

Figure 15: Influence of the electromagnet on the vertical displacement of the carrier.

3.4 Magnetic rail with propulsion function

Figure 16 shows thrust force generated by the electromagnet. Dependence of the levitation gap on current of the electromagnet in Configuration I and II at gradient of the electromagnet 30 degree is shown. Configuration I shows larger displacement than Configuration II. From Figure 16, Configuration I shows larger thrust force than Configuration II. As gradient of the electromagnet in Configuration II changes, distance between the electromagnet and the rail on the ground increases. In Configuration I, the larger the levitation gap is, the smaller thrust force is. But when the gradient of the frame increases, larger thrust force is expected in Configuration I. The thrust force occurred by the gradient of the frame as well as by the repulsive force of the electromagnet is confirmed. The thrust force was not still enough large in both methods. The configuration for the larger thrust force is considered.

Figure 17 shows method for the propulsion using the rail with propulsion function. The interaction force between the electromagnet and the permanent magnet is utilized.

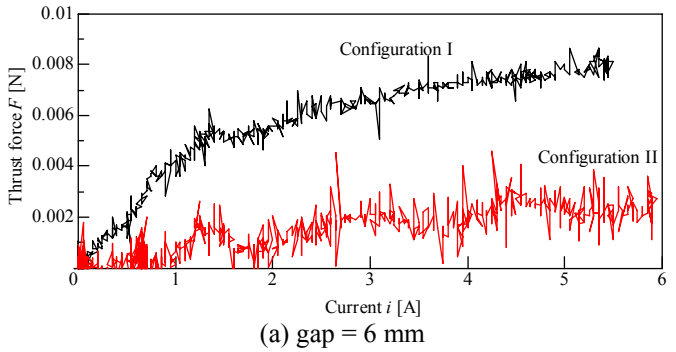

(a) gap = 6 mm

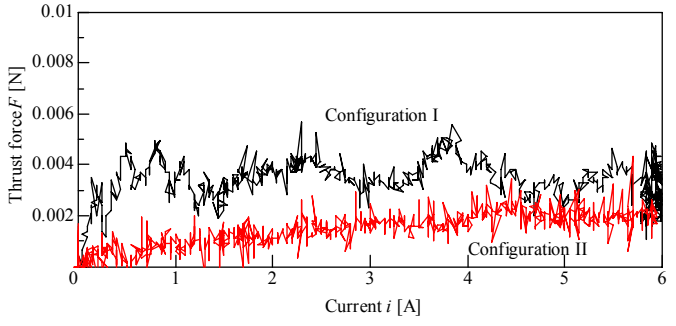

(b) gap = 9 mm

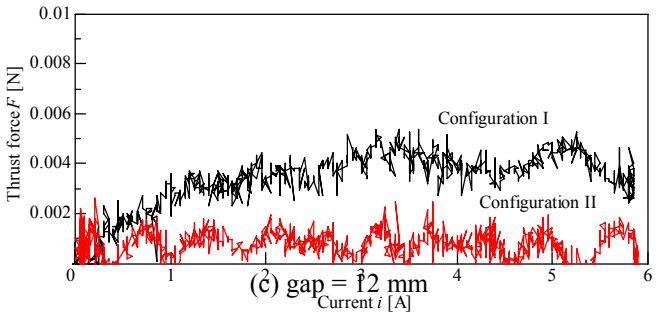

(c) gap = 12 mm

Figure 16: Thrust force of the electromagnet (Configuration I and II.

Electromagnets are installed on the part of surface of the rail. The electromagnet makes magnetic slope on the rail. The magnetic slope acts the permanent magnet of the load carrier, and thrust force occurs. In the rail with propulsion function, levitation gap of the carrier is not directly changed. So influence of thrust force on the HTSC is small. Figure 18 shows configuration of the propulsion rail. The electromagnets are installed on the surface of the rail. To get the space for electromagnets, additional magnet is set on the side of the previous permanent magnet. As a result, vertical flux density distribution shifts 9 mm for upper direction. This means that levitation gap 3 mm in Configuration I and II contains 12 mm in the new propulsion rail. The current of the electromagnet on surface of the rail is controlled to generate thrust force. In this paper, ON-OFF switching control for the electromagnet current is used.

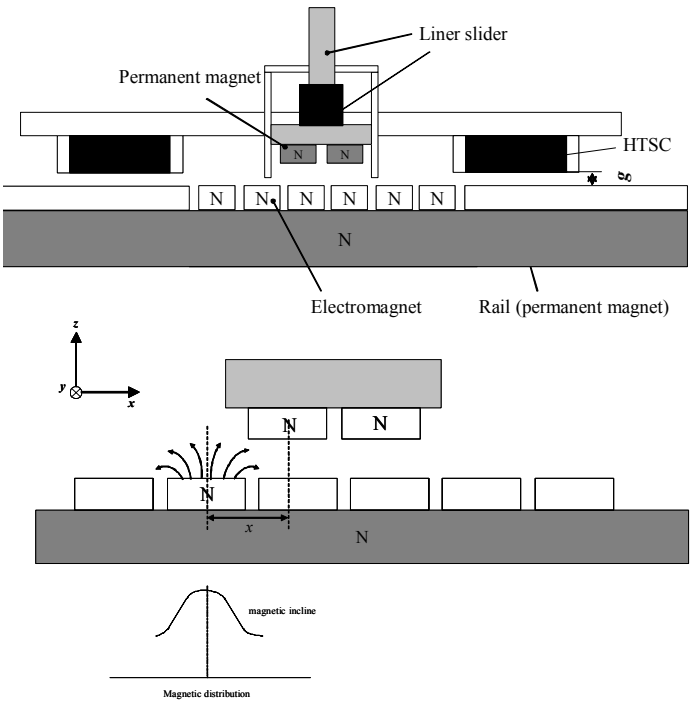

Figure 17: Method for propulsion (magnetic rail).

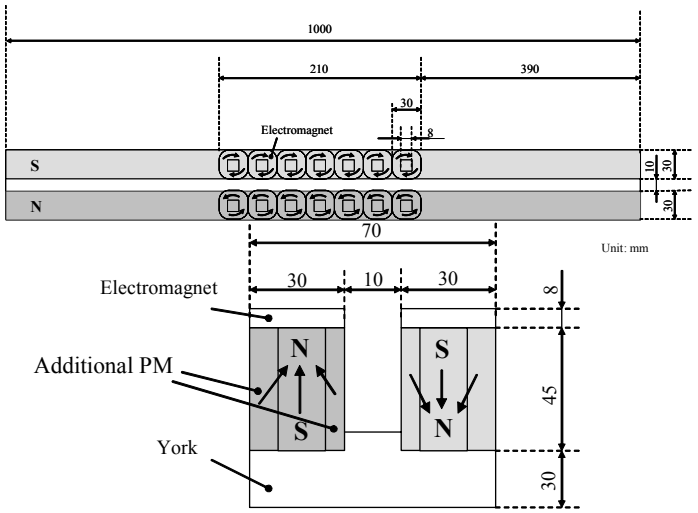

Figure 18: Configuration of the propulsion rail.

Figure 19 shows dependence of the load weight on the thrust force in Configuration I and II. Static force is measured by a load cell. Current of the electromagnet is 10.0 A. As shown in Figure 16, Configuration It shows better thrust characteristics than Configuration II. In these configurations, position of the load stage has little influence on thrust force. So dependence of load weight on thrust force is small. Figure 20 shows that in propulsion rail system. Results when current of the electromagnet is 2.5 A and 5.0 A are shown. As shown in Figure 17 and 18, thrust force is given by the interaction between permanent magnet under the load stage and electromagnet on surface of the rail. Distance between this permanent magnet and electromagnet becomes small at a larger load. As a result, thrust force at a larger load becomes large and is in propulsion to the weight value square. Compared with Configuration I and II, it is shown that propulsion rail shows larger thrust force. We introduce this propulsion method for the hybrid conveyance system.

Figure 21 shows running speed of the carrier. In this experiment, only two electromagnets are excited to generate the thrust force because of the limitation of power supply. Although running speed at i = 2.5 A is small, enough speed is given at i = 5.0 A.

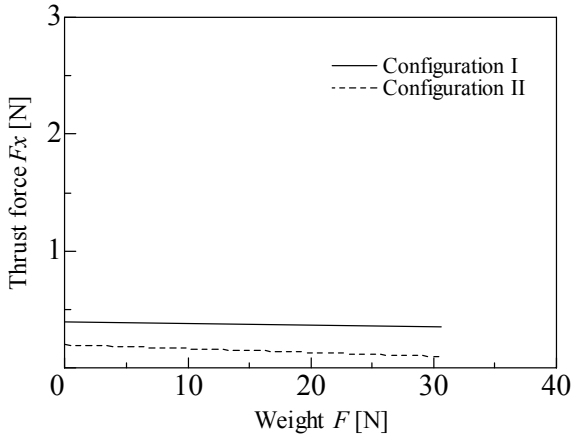

Figure 19: Dependence of load weight on static thrust force in Configuration I and II.

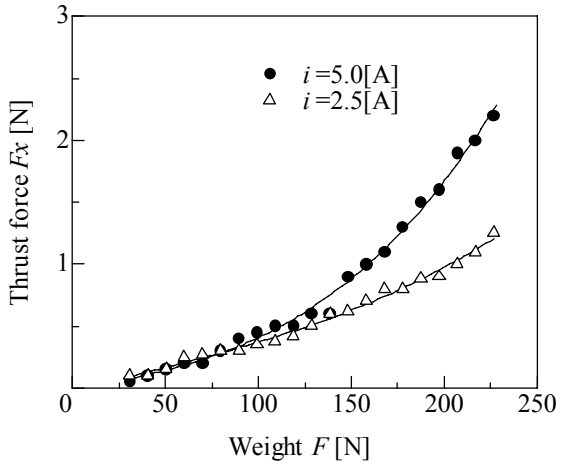

Figure 20: Dependence of load weight on static thrust force in propulsion rail system.

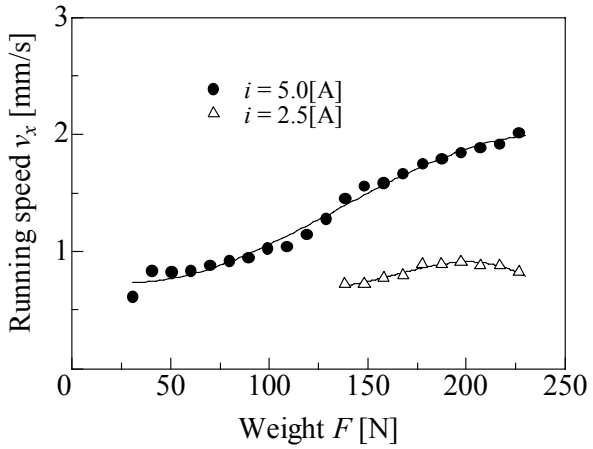

Figure 21: Dependence of load weight on running speed of the carrier in propulsion rail system.

4 CONCLUSION

We have developed the hybrid conveyance system that guidance is obtained by pining force of the HTSC and levitation force by the permanent magnet. Method of the propulsion is discussed. The system additional electromagnet installed on the carrier is considered. In displacement of the levitating direction and damping characteristic, there is a little influence on pining force of the HTSC. The configuration for the larger thrust force should be considered. The propulsion method by using the rail with propulsion function is proposed. Design for the propulsion rail system is shown.

This propulsion rail shows better thrust force characteristic. Compared with previous propulsion method, the influence on pining force of the HTSC in propulsion rail system is small.

Part of this research was financially supported by the Kansai University Grant-in-Aid for progress of research in graduate course, 2005.

REFERENCES

Cardwell, D.A. & Campbell, A.M., 1997. Dynamic Properties of Superconducting Magnetic Bearings, *IEEE Trans. on Applied Superconductivity,* 7(2):924-927.

Dodo, D. & Ohashi, S. 2005. Propulsion Method for the Magnetically Levitated Hybrid Conveyance System. *Proc. 5th intern. symp. on Linear Drives for Industry Applications (LDIA2005), Kobe, Japan, 2005*.437-440.

Moon, F.C. 1994. *Superconducting Levitation,* Wiely New York, U.S.A.

Ohashi, S, Ito, T. & Hirane, H. 1999. The Basic Characteristics of the Pinning Force and Flux Density Distribution of the HTSC-Permanent Magnet Hybrid Bearing. *Proc. 10th intern. symp. on Superconductivity (ISS99), Morioka, Japan, 1999*.794-796.

Ohashi, S., Tanaka, H. & Hirane, H. 2001. Three Dimensional Vibration of the HTSC-Permanent Magnet Bearing System in the Mechanical Resonant State", *IEEE Trans. on Applied Superconductivity,* 11(1):1812-1815.